

## Direct Preparation and Size Control of Highly Crystalline Cubic ITO Nanoparticles in a Concentrated Solution System

Yosuke Endo, Takafumi Sasaki, Kiyoshi Kanie,\* and Atsushi Muramatsu\*

*Institute of Multidisciplinary Research for Advanced Materials, Tohoku University, 2-1-1 Katahira, Aoba-ku, Sendai 980-8577*

(Received September 30, 2008; CL-080941; E-mail: kanie@tagen.tohoku.ac.jp, mura@tagen.tohoku.ac.jp)

Highly crystalline cubic indium tin oxide (ITO) nanoparticles with narrow size distribution were successfully prepared directly in one step from a mixed solution of indium and tin salts by a solvothermal method with ethylene glycol as solvent. Also, size was easily manipulated by changing conditions, such as aging period and sodium hydroxide concentration.

Tin-doped indium oxide (ITO), an n-type transparent conducting oxide (TCO), has been extensively investigated owing to many ITO applications as typified by flat panel display technology and electrical paper, which utilize the unique properties of high optical transparency of ITO in the visible region and controllable low resistivity.<sup>1</sup> The direct preparation of ITO nanoparticles with high crystallinity, homogeneous composition, and well-defined particle morphologies with narrow size distributions is of particular technological interest. Preparation methods of  $\text{In}_2\text{O}_3$  or ITO particles have been reported based on the combination of coprecipitation of metal precursors and successive thermal treatment,<sup>2</sup> laser-induced fragmentation,<sup>3</sup> solvothermal synthesis,<sup>4</sup> microwave-assisted synthesis,<sup>5</sup> emulsion techniques,<sup>6</sup> chemical vapor deposition,<sup>7</sup> and one-pot preparation of colloids.<sup>8</sup> However, the precise control of ITO fine particles in size, shape, and structure simultaneously has never been reported, mainly because of the difficulty in the strict separation of nucleation and growth, and crystallization at rather low temperature, below 300 °C. Removal of water from the reaction systems also brings complication of the preparation procedures.<sup>2</sup>

In the present study, we will report herein the investigation of morphology and size control of ITO nanoparticles. In particular, we have succeeded in one-step preparation of cubic ITO nanoparticles with high crystallinity by a solvothermal method using ethylene glycol (EG) as solvent. The particle preparation was carried out by the addition of a nonaqueous EG solution of NaOH (1.0–2.0 M) to the same volume of an EG solution of  $\text{InCl}_3 \cdot 4\text{H}_2\text{O}$  and  $\text{SnCl}_4 \cdot 5\text{H}_2\text{O}$  at 0 °C under agitation. Concentration of the  $\text{InCl}_3$  and  $\text{SnCl}_4$  mixed precursor solution in EG was adjusted to 0.50 and 0.050 M, respectively. After stirring for 15 min, 10 mL of the suspension was transferred into a 23-mL Teflon-lined autoclave and aged at 250 °C for 4 days. Obtained particles were collected by centrifugation (18000 rpm, 10 min) and washed three times with ethanol. The product phase and morphology were characterized by X-ray diffraction analysis (XRD), and transmission electron microscopy (TEM).

First, the effect of NaOH concentration on the particle morphology and size in this system was investigated. Figure 1 shows the TEM images of the ITO nanoparticles obtained with different concentration of NaOH ((a): 2.0 M; (b): 1.5 M; and (c): 1.0 M). Cubic-shaped ITO nanoparticles were obtained as dark blue powders under all the conditions. As shown in Figure 1, the particle size was successfully controlled by decreasing the initial

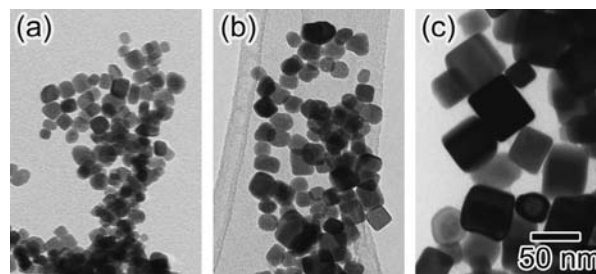


**Figure 1.** TEM images of ITO nanoparticles obtained with changing of the NaOH concentration. (a): 2.0 M; (b): 1.5 M; and (c): 1.0 M. The scale bar in (c) is common for all images.

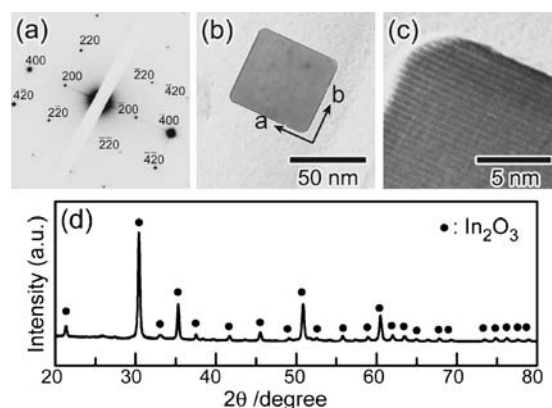


**Figure 2.** Selected-area electron diffraction (a), respective TEM images (b), and HRTEM (c) of ITO nanoparticles shown in Figure 1c and the XRD pattern (d).

NaOH concentrations. The particle mean sizes and the size distributions are  $15.1 \pm 2.9$ ,  $20.3 \pm 3.5$ , and  $43.5 \pm 10.3$  nm, respectively. The decrease in size with increasing NaOH concentration was due to the increase in number of nuclei formed. Generally speaking, the rather higher alkaline condition is advantageous to the formation of the monomer, precursor complex, of metal oxide.<sup>9</sup>

ITO nanoparticles with various Sn concentrations were also prepared with different initial molar ratios of Sn/In from 0 to 0.15. In all cases,  $\text{In}_2\text{O}_3$  and ITO nanoparticles with cubic crystal structures were obtained; however the formation of trace  $\text{SnO}_2$  was also found in the case of Sn/In = 0.15 by XRD measurement. On the other hand, it was confirmed that Sn/In molar ratio in one ITO particle prepared at Sn/In = 0.10 was the same as the initial feed ratio by energy dispersive X-ray (EDX) analysis.

Figure 2 shows the TEM, high-resolution TEM (HRTEM) images, the electron diffraction (ED) spots of ITO nanoparticles, and XRD pattern of the ITO nanoparticles shown in Figure 1c.

The ED spots as well as HRTEM analyses of the one particle shown in Figure 2a revealed that the crystal structure of the cubic-shaped ITO nanoparticles is basically single-crystalline, and the lattice parameter of the  $a$  axis of the resulting particle can be assigned as 1.014 nm. The length is quite similar to the  $a$  axis of  $\text{In}_2\text{O}_3$  with a cubic crystal structure (JCPDS No 06-0416) of 1.012 nm. Thus the incorporation of Sn ions into the crystal structure of  $\text{In}_2\text{O}_3$  does not influence the lattice parameter. However, streaks in the direction towards the  $a$  and  $b$  axes are observed as shown in Figure 2a. The streaks might be derived from incorporation of Sn ions and existence of oxygen vacancy in the crystal.

The effect of solvents on the ITO synthesis was also investigated. Figures 3 and 4 show the TEM images and XRD patterns of the particles obtained in (a): EG; (b): diethylene glycol (DEG); (c): 80% aqueous EG solution; and (d): butanol (BuOH), respectively. Here, the molar ratios of  $\text{In}^{3+}/\text{OH}^-$  and Sn/In were fixed as 1/3 and 0.10, respectively, with other things in the standard conditions, but aging time was 12 h. As shown in Figure 3a, irregularly shaped ITO nanoparticles are obtained in EG aged for 12 h, and the particle size is ca. 10 nm. In the case of DEG, ITO nanoparticles are also formed as a single phase, and the particle shape is basically cubic and the size is about 20 nm. In contrast, the diffraction peaks of colorless powder obtained in an 80 wt % aqueous EG solution system (Figure 4c) are indexed to be an indium oxyhydroxide (InOOH).

As a result of the comparison of EG–water and EG alone systems, the addition of water seems inhibitory to the formation of ITO crystals. In the aqueous solution system of indium

salts, the formation of InOOH was strongly enhanced. One might consider that InOOH once formed during the reaction is hardly converted into  $\text{In}_2\text{O}_3$  phase, because of extremely low solubility. In other words, InOOH cannot play a role as an intermediate for  $\text{In}_2\text{O}_3$  formation. The solid particles obtained by using BuOH as a solvent consist of  $\text{In}_2\text{O}_3$  and InOOH. It shows stepwise phase transition from metal hydroxides to oxides through oxyhydroxides by the dissolution–precipitation in the case of the BuOH system. This behavior is commonly observed in aqueous systems to form metal oxides.<sup>10</sup> In contrast, in the solvothermal system as shown here, direct formation of ITO solid particles is observed starting from amorphous indium hydroxides,  $\text{In}(\text{OH})_3$  and InOOH phases are not detected as intermediates.

In conclusion, highly crystalline cubic-shaped ITO nanoparticles were successfully prepared in one step via solvothermal reaction with EG and DEG as solvents. Furthermore, we have succeeded in the stepwise size control of ITO nanocubes with changing In/OH molar ratio. In this case, formation of ITO phase was inhibited by the contained water in the solvent owing to formation of InOOH. Further study concerning the formation mechanism of the cubic single-crystalline ITO nanoparticles is now in progress, and it would lead to the development of the preparation of monodispersed single-crystalline ITO nanoparticles with high conductivity, which is applicable to TCO.

This work was financially supported by METI & NEDO Rare Metal Substitute Materials Development Project.

## References

- 1 a) H. L. Hartnagel, A. L. Dawar, A. K. Jain, C. Jagdish, *Semiconducting Transparent Thin Films*, IOP Publishing, Bristol, **1995**. b) I. Hamberg, C. G. Granqvist, *J. Appl. Phys.* **1986**, *60*, R123.
- 2 a) J. E. Song, D. K. Lee, H. W. Kim, Y. I. Kim, Y. S. Kang, *Colloids Surf., A* **2005**, *257–258*, 539. b) K. Y. Kim, S. B. Park, *Mater. Chem. Phys.* **2004**, *86*, 210.
- 3 H. Usui, T. Sasaki, N. Koshizaki, *J. Phys. Chem. B* **2006**, *110*, 12890.
- 4 a) J.-S. Lee, S.-C. Choi, *J. Eur. Ceram. Soc.* **2005**, *25*, 3307. b) J. Yang, C. Li, Z. Quan, D. Kong, X. Zhang, P. Yang, J. Lin, *Cryst. Growth Des.* **2008**, *8*, 695.
- 5 M. Okuya, N. Ito, K. Shiozaki, *Thin Solid Films* **2007**, *515*, 8656.
- 6 P. Sujatha Devi, M. Chatterjee, D. Ganguli, *Mater. Lett.* **2002**, *55*, 205.
- 7 Y. Li, C. H. Ye, L. Yang, C. Wang, C. R. Zheng, L. D. Zhang, *Chem. Lett.* **2007**, *36*, 442.
- 8 a) W. S. Seo, H. H. Jo, K. Lee, J. T. Park, *Adv. Mater.* **2003**, *15*, 795. b) Q. Liu, W. Lu, A. Ma, J. Tang, J. Lin, J. Fang, *J. Am. Chem. Soc.* **2005**, *127*, 5276. c) C. H. Lee, M. Kim, T. Kim, A. Kim, J. Paek, J. W. Lee, S.-Y. Choi, K. Kim, J.-B. Park, K. Lee, *J. Am. Chem. Soc.* **2006**, *128*, 9326. d) W. Zhang, Z. Huang, T. Li, Q. Tang, D. Ma, Y. Qian, *Chem. Lett.* **2005**, *34*, 118.
- 9 a) T. Sugimoto, M. M. Khan, A. Muramatsu, *Colloid Surf., A* **1993**, *70*, 167. b) T. Sugimoto, A. Muramatsu, *J. Colloid Interface Sci.* **1996**, *184*, 626. c) K. Kanie, A. Muramatsu, S. Suzuki, Y. Waseda, *Mater. Trans.* **2004**, *45*, 1.
- 10 T. Sugimoto, K. Sakata, A. Muramatsu, *J. Colloid Interface Sci.* **1993**, *159*, 372.

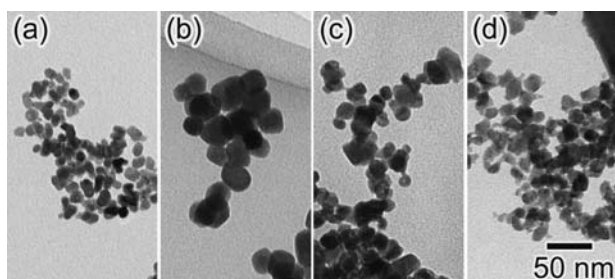


**Figure 3.** TEM images of particles obtained in (a): EG; (b): DEG; (c): 80 wt % aqueous EG solution; and (d): BuOH. The scale bar in (d) is common for all images.

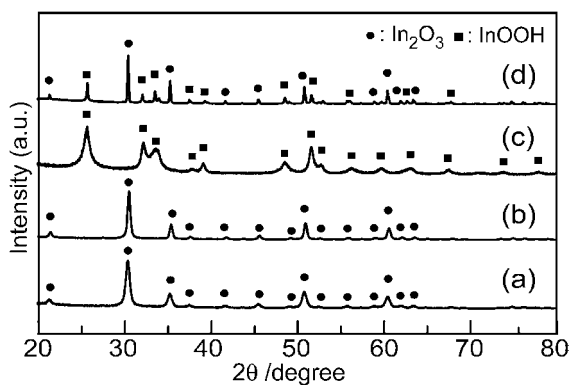


**Figure 4.** XRD patterns of particles obtained in (a): EG; (b): DEG; (c): 80 wt % aqueous EG solution; and (d): BuOH.